

Pancreatic Microcirculation Profiles in the Progression of Hypertension in Spontaneously Hypertensive Rats

Mingming Liu,^{1,2,*} Xiaohong Song,^{1,*} Bing Wang,¹ Yuan Li,¹ Ailing Li,¹ Jian Zhang,^{1,2} Honggang Zhang,¹ and Ruijuan Xiu¹

BACKGROUND

Emerging evidence indicates that the pancreas serves as a major source of degrading protease activities and that uncontrolled proteolytic receptor cleavage occurs under hypertensive conditions, which leading to systemic dysfunction and end-organ damage. However, changes in pancreatic microcirculation profiles during the progression of hypertension remain unknown.

METHODS

Pancreatic microcirculatory blood distribution patterns and microvascular vasomotion of spontaneously hypertensive rats (SHRs) and normotensive control Wistar Kyoto rats at 5, 8, 13, and 18 weeks of age were determined. Wavelet transform analysis was performed to convert pancreatic microhemodynamic signals into time–frequency domains and construct 3-dimensional spectral scalograms. The amplitudes of characteristic oscillators including endothelial, neurogenic, myogenic, respiratory, and cardiac oscillators were compared among groups. Plasma nitrite/nitrate levels were measured using a Griess reaction. Additionally, endothelin-1, malondialdehyde, superoxide dismutase, and interleukin-6 levels were determined by enzyme-linked immunosorbent assay.

RESULTS

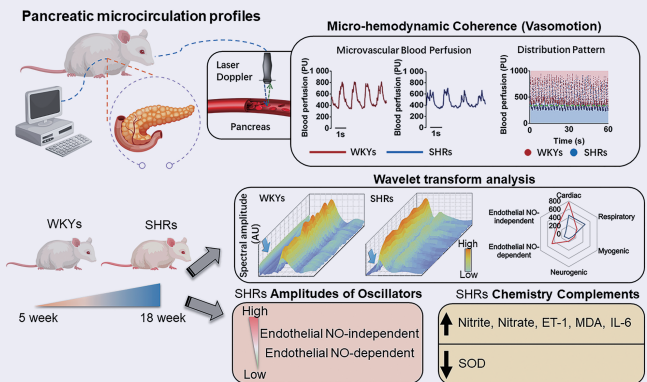
SHRs exhibited a reduced blood distribution pattern with progressively decreased average blood perfusion, amplitude, and frequency of microvascular vasomotion. Wavelet transform spectral analysis revealed significantly reduced amplitudes of endothelial oscillators from 8- to 18-week-old SHRs. Additionally, the blood microcirculatory chemistry complements explained the microhemodynamic profiles partially, as demonstrated by an increase in plasma nitrite/nitrate, endothelin-1,

malondialdehyde, and interleukin-6 levels and a decreased superoxide dismutase level in SHRs.

CONCLUSIONS

Pancreatic microcirculation profiles are abnormal in the progression of hypertension in SHRs, including a disarranged blood distribution pattern, impaired microvascular vasomotion, and reduced amplitudes of endothelial oscillators.

GRAPHICAL ABSTRACT



Keywords: blood distribution pattern; blood pressure; hypertension; microcirculation profiles; microvascular vasomotion; oscillator

doi:10.1093/ajh/hpaa164

Hypertension is characterized by elevated blood pressure and irregular peripheral vascular resistance regulation and is caused by multiple factors, including genetic susceptibility and

environmental exposure; moreover, it is one of the most widespread cardiovascular diseases.¹ In clinical practice, hypertension is not a single disease and instead encompasses various

Correspondence: Honggang Zhang (zhanghg1966126@163.com).

Initially submitted December 25, 2019; date of first revision September 29, 2020; accepted for publication October 2, 2020; online publication October 15, 2020.

¹Institute of Microcirculation, Chinese Academy of Medical Sciences & Peking Union Medical College, Key Laboratory of Microcirculation, Ministry of Health, Beijing, China; ²Diabetes Research Center, Chinese Academy of Medical Sciences, Beijing, China.

*These authors contributed equally to this study.

© The Author(s) 2020. Published by Oxford University Press on behalf of American Journal of Hypertension, Ltd. This is an Open Access article distributed under the terms of the Creative Commons Attribution Non-Commercial License (<http://creativecommons.org/licenses/by-nc/4.0/>), which permits non-commercial re-use, distribution, and reproduction in any medium, provided the original work is properly cited. For commercial re-use, please contact journals.permissions@oup.com

clinical features, such as hyperglycemia, insulin resistance, and capillary rarefaction. Additionally, hypertension has a dramatic impact on the incidence and progression of cardiovascular events and microvascular complications. However, the pathogenesis of hypertension has not yet been fully clarified.

There has been increasing attention on the association between microcirculation and hypertension during the last decade.² The microcirculation, structurally consisting of microvascular endothelial cells, is necessary to provide nutrients and remove metabolites matching metabolic demand and plays a crucial role in maintaining the physiological function of organs.³ Moreover, the microcirculatory system has been implicated in the regulation of blood pressure.⁴ Defined as the spontaneous oscillation of microcirculatory tone occurring in microvessel beds, microvascular vasomotion has been demonstrated to be capable of adjusting blood perfusion.⁵ In our previous study, we showed a microhemodynamic pathological phenotype of pancreatic islet microcirculation in 8-week-old spontaneously hypertensive rats (SHRs), which revealed a temporal link between hypertensive conditions and microcirculatory abnormalities and indicated an association between microvascular vasomotion and the execution of functional units (microvascular endothelial cells).⁶ Therefore, microcirculatory dysfunction is associated with abnormal peripheral resistance and irregular organic blood perfusion.⁷

Recently, it has been demonstrated that uncontrolled proteolytic receptor cleavage occurs in microcirculation in hypertension patients, leading to cellular and systemic dysfunction and even end-organ damage.^{8–10} It has been proven that the pancreas serves as a major systemic major source of digestive enzymes (mainly serine proteases,¹¹ such as matrix metalloproteinases^{12,13} and trypsin¹⁴) in the microcirculation and surrounding tissues,¹⁵ which may be one of the explanations underlying enhanced protease activity in SHRs¹⁶ and the generated pathophysiological response of clinical manifestations observed in hypertensive individuals. These lines of evidence highlight the importance of pancreatic microcirculation in the development of hypertension.

Analyses of pancreatic microcirculation profiles are a reasonable strategy for investigating changes in pancreatic microcirculation. We recently established a method for assessing pancreatic microcirculation profiles by microhemodynamic and microcirculatory blood distribution patterns.¹⁷ In addition, the amplitudes of characteristic microcirculatory oscillators should be enrolled into microcirculation profiles considering the fundamental role of these oscillators. To the best of our knowledge, there is little information on the pancreatic microcirculation profiles in the progression of hypertension. Therefore, the aim of the current study was to investigate the changes in pancreatic microcirculation profiles in SHRs and their normotensive control Wistar Kyoto rats (WKYs) ranging from prehypertensive to hypertensive stages.

METHODS

Animals

This study was approved by the Institutional Animal Care and Use Committee (IACUC) at Chinese Academy

of Medical Sciences (CAMS) and all experiments were performed in accordance with the guidelines for the Care and Use of Laboratory Animals (IACUC-201709). Male 5-, 8-, 13-, and 18-week-old SHRs and normotensive control WKYs ($n = 6$ each group) were provided by Vital River Laboratory Animal Technology (Beijing, China). All rats were housed separately in cages at a temperature of 22 °C and 55%–70% humidity under a light–dark cycle (12 hour light–12 hour dark), with unlimited access to standard rodent chow diet and water.

Measurement of blood pressure

Blood pressure was measured by a computerized rat occlusion tail-cuff blood pressure device BP-2010A (Softron Biotechnology, Beijing, China). Briefly, rats were placed into a restraint box over a heating pad (TMC-213) preheated to 37 °C. Then, the occlusion tail cuff was connected to the sensor (BP98-RCP-M, Softron Biotechnology). After 5 minutes of acclimatization, the systolic blood pressure, diastolic blood pressure, and mean arterial pressure of the rats were recorded. The measurements were repeated 3 times.

Determination of pancreatic microcirculation profiles

The pancreatic microcirculation profiles were determined with a laser Doppler blood perfusion monitoring system (Moor Instrument, Axminster, UK), according to the Doppler frequency shift principle.¹⁸ After acclimatization, rats were anesthetized with 2% inhaled isoflurane in a 50% mixture of oxygen. A planned incision was made around the medioventral line to expose the pancreas. Laser Doppler signals of pancreatic microcirculation were captured by VP4s probe. To describe the microcirculatory distribution pattern, the microvascular blood perfusion unit (PU) was illustrated in a scatter plot. The changes in microhemodynamic parameters, including average blood perfusion, velocity, amplitude, and frequency, were analyzed by Moor VMS PC 3.1. The average microvascular blood perfusion was calculated as the total microvascular blood perfusion divided by min, while the velocity was captured according to the changes in scattered light intensity of standard microparticles. Furthermore, the frequency and amplitude were calculated as the number of peaks that occurred per min and the difference between the minimum PU and maximum PU (Δ PU), respectively.

Wavelet transform spectral analysis

The combination of laser Doppler flowmetry with wavelet transform signal processing analysis is capable of revealing oscillations in microcirculation that relate to physiological phenomena. Therefore, wavelet transform was performed to convert microhemodynamic signals into the time–frequency domain, revealing the contributions of biological oscillators to microcirculatory changes. Considering the commonly used frequency intervals applied to investigate the microcirculatory function in humans and experimental animals, the frequency spectrum was divided into a set of frequency

Table 1. General blood pressure of SHR and WKYs

Age (weeks)	Groups	Blood pressure		
		SBP (mm Hg)	MAP (mm Hg)	DBP (mm Hg)
5	WKYs	109.00 ± 1.55	87.20 ± 4.18	76.80 ± 6.03
	SHRs	112.80 ± 1.02	91.20 ± 2.08	81.80 ± 2.42
8	WKYs	113.30 ± 2.72	92.67 ± 3.49	82.67 ± 4.11
	SHRs	138.30 ± 2.01 [#]	112.50 ± 2.38 [#]	98.17 ± 2.75 [*]
13	WKYs	133.80 ± 2.47	109.30 ± 1.87	96.17 ± 2.02
	SHRs	176.20 ± 4.62 [#]	147.20 ± 3.76 [#]	133.20 ± 5.55 [#]
18	WKYs	140.00 ± 1.24	119.00 ± 1.55	108.00 ± 1.90
	SHRs	210.00 ± 4.03 [#]	184.00 ± 2.88 [#]	172.50 ± 3.51 [#]

Abbreviations: DBP, diastolic blood pressure; MAP, mean arterial pressure; SBP, systolic blood pressure; SHRs, spontaneously hypertensive rats; WKYs, Wistar Kyoto rats.

^{*}*P* < 0.05 compared with WKYs.

[#]*P* < 0.01 compared with WKYs.

bands—0.01–0.015, 0.015–0.04, 0.04–0.15, 0.15–0.4, 0.4–2, and 2–5 Hz,^{19–21} and attributed to NO-independent endothelial and NO-dependent endothelial, neurogenic, myogenic, respiratory, and cardiac oscillators, respectively. To further investigate the microhemodynamic spectrum, the Morlet wavelet was scaled to provide a Gaussian window that is shifted along time and frequency domains,²² and spectral amplitudes were calculated by averaging wavelet coefficients to obtain the time–frequency spectral characteristics of those oscillators. A three-dimensional (3-D) amplitude spectral scalogram was constructed based on the wavelet transformed microhemodynamic data. Variants including time (seconds), frequency (Hz), and spectral amplitude (AU) were located in the coordinates. The amplitudes of 6 oscillators were compared between WKYs and SHRs at 5, 8, 13, and 18 weeks.

Enzyme-linked immunosorbent assays (ELISAs)

Compared with NO level, plasma nitrite/nitrate levels are amenable to the routine collection, storage, and measurement. Therefore, plasma nitrite/nitrate levels instead of NO levels were selected as microcirculation-related chemistry complements. Plasma nitrite/nitrate concentrations of WKYs and SHRs were measured using a Griess reaction assay kit (R&D Systems, MN). Moreover, plasma superoxide dismutase (Blue Gene Biotech, Shanghai, China), malondialdehyde (Blue Gene Biotech), interleukin-6 (Blue Gene Biotech), and endothelin-1 (R&D Systems) levels of WKYs and SHRs at all ages were determined by ELISA kits following the manufacturer's protocols. The optical density was recorded by a microplate reader (Thermo Scientific Multiskan GO, MA). All plasma samples were assayed in duplicate.

Statistical analysis

All statistical analyses were performed using SPSS software (version 21.0 for Windows, SPSS, Chicago, IL), and laser Doppler signals and wavelet analysis data were presented as arithmetic means ± SEM. Comparisons of

pancreatic microcirculation profiles in different groups were conducted by Student's *t*-test, and a *P* value of less than 0.05 was considered statistically significant. The correlations were established by calculating Pearson's correlation coefficient (*r*) and were considered relevant for associated *P* < 0.05 and values of *r* > 0.3 or < −0.3.

RESULTS

Pancreatic microcirculation profiles in WKYs and SHRs

To investigate the changes in pancreatic microcirculation profiles in the progression of hypertension, animals in the early stage (5 weeks) of hypertension were included in the analysis. The blood pressures of SHRs and WKYs at different ages are shown in Table 1. Notably, the systolic blood pressure of SHRs at 5 weeks was in the normal range, and SHRs had significantly higher systolic blood pressure, diastolic blood pressure, and mean arterial pressure than WKYs at 8, 13, and 18 weeks, which gradually increased with the progression of hypertension. The laser Doppler flowmetry dataset revealed that SHRs and WKYs exhibited distinctly different pancreatic microcirculatory vasomotion (Figure 1a) and blood distribution patterns (Figure 1b) at different weeks.

Under normotensive conditions, WKYs presented stable biorhythmic contraction and relaxation with a regular and higher blood distribution pattern scale; in contrast, SHRs exhibited a disarranged pancreatic microcirculatory oscillation and a lower blood perfusion pattern scale, even in the normotensive stage at 5 weeks. Quantification data of pancreatic microcirculation profiles are illustrated in Figure 1c. SHRs showed a significant decrease in average blood perfusion at all stages of hypertensive progression. Moreover, both the amplitude and frequency of microvascular vasomotion were significantly decreased in 8-, 13-, and 18-week-old SHRs. The velocity was significantly reduced in 5-, 8-, and 18-week-old SHRs, indicating deteriorating pancreatic microcirculation profiles throughout the progression of hypertension.

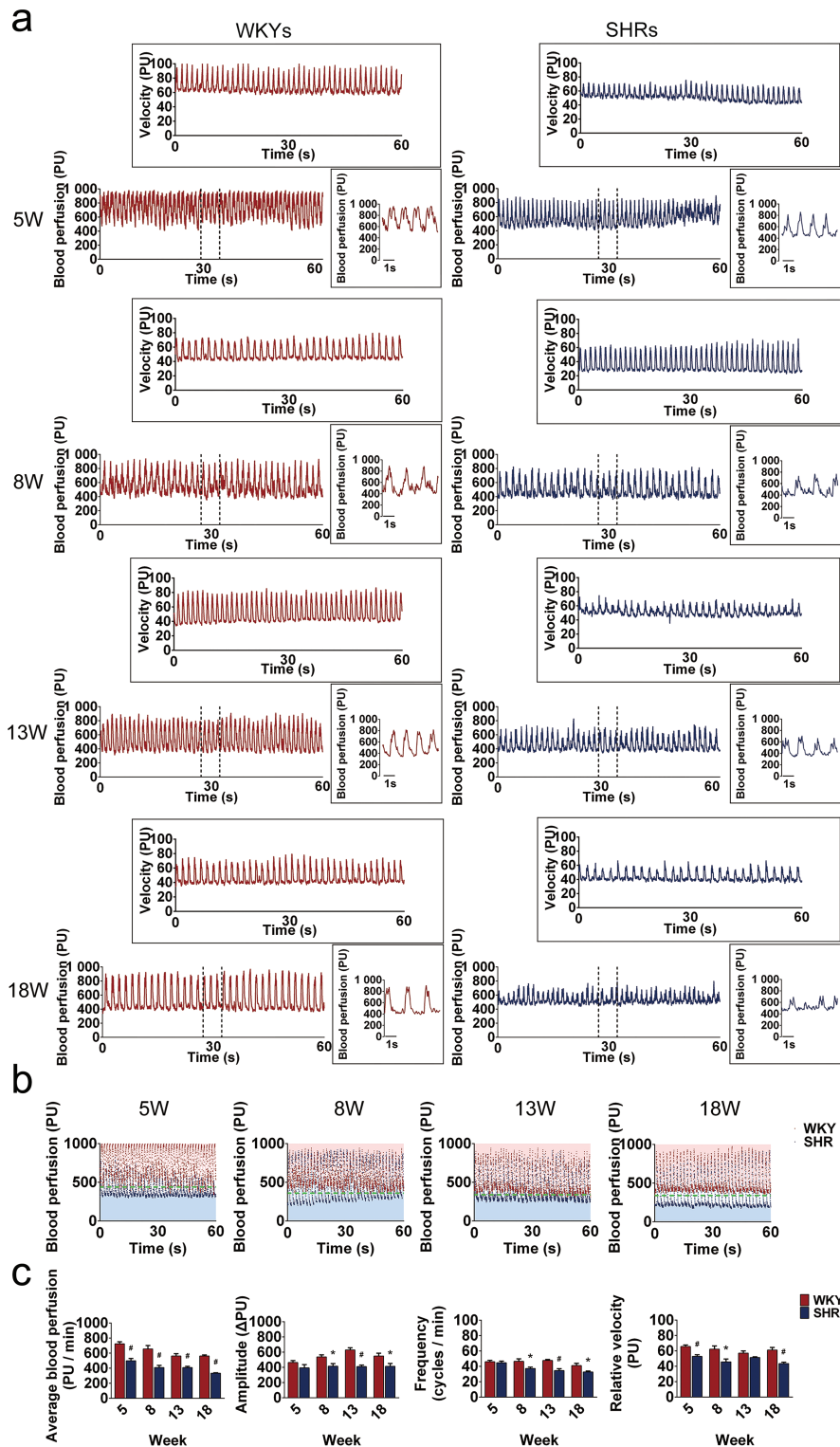


Figure 1. Pancreatic microcirculation profiles in the progression of hypertension. **(a)** Pancreatic microvascular vasomotion of WKYs and SHRs. The velocity was extracted in the rectangular insert. The microcirculatory blood perfusion between dashed lines (5 seconds) is illustrated in the square insert. **(b)** Pancreatic microcirculatory blood distribution pattern of WKYs and SHRs. The red dot represents WKY. The blue dot represents SHR. The green dashed line represents the boundary of the microcirculatory blood distribution pattern between WKYs and SHRs. **(c)** Quantification analysis of pancreatic microhemodynamic data including average blood perfusion (PU/minutes), relative velocity (PU), amplitude (Δ PU), and frequency (cycles/minutes) of WKYs and SHRs at 5, 8, 13, and 18 weeks. All data are presented as the mean \pm SEM. * $P < 0.05$ compared with WKYs, # $P < 0.01$ compared with WKYs. The red line and dots, microcirculatory data of WKYs. The blue line and dots represent SHRs. Abbreviations: PU, perfusion unit; SHR, spontaneously hypertensive rat; WKY, Wistar Kyoto rat.

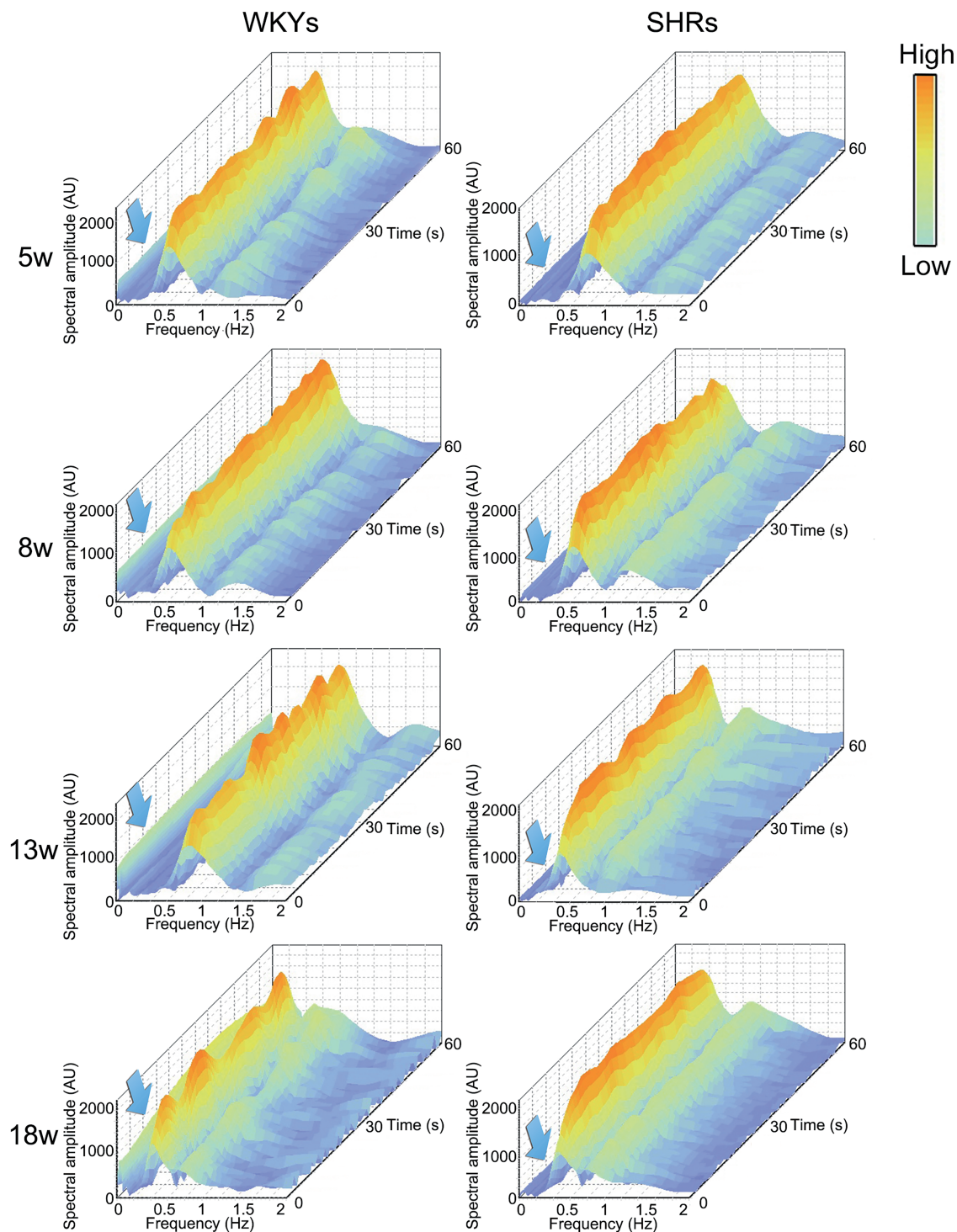


Figure 2. 3-D characteristic amplitude spectral scalograms of pancreatic microcirculation profiles. 3-D time–frequency spectral scalograms derived from pancreatic microcirculation profiles data corresponding to microcirculatory blood perfusion signals in SHRs and WKYs at 5, 8, 13, and 18 weeks were illustrated utilizing wavelet coefficients. Microhemodynamic variants, including time (seconds), frequency (Hz), and spectral amplitude (AU), were located in the coordinates. The gradient colored scalogram ranging from dark blue (low energy) to light orange (high energy) represents an energy continuous wavelet coefficient and spectral amplitudes. Arrows indicate the frequencies characterized by endothelial oscillators. Abbreviations: SHRs, spontaneously hypertensive rats; WKYs, Wistar Kyoto rats.

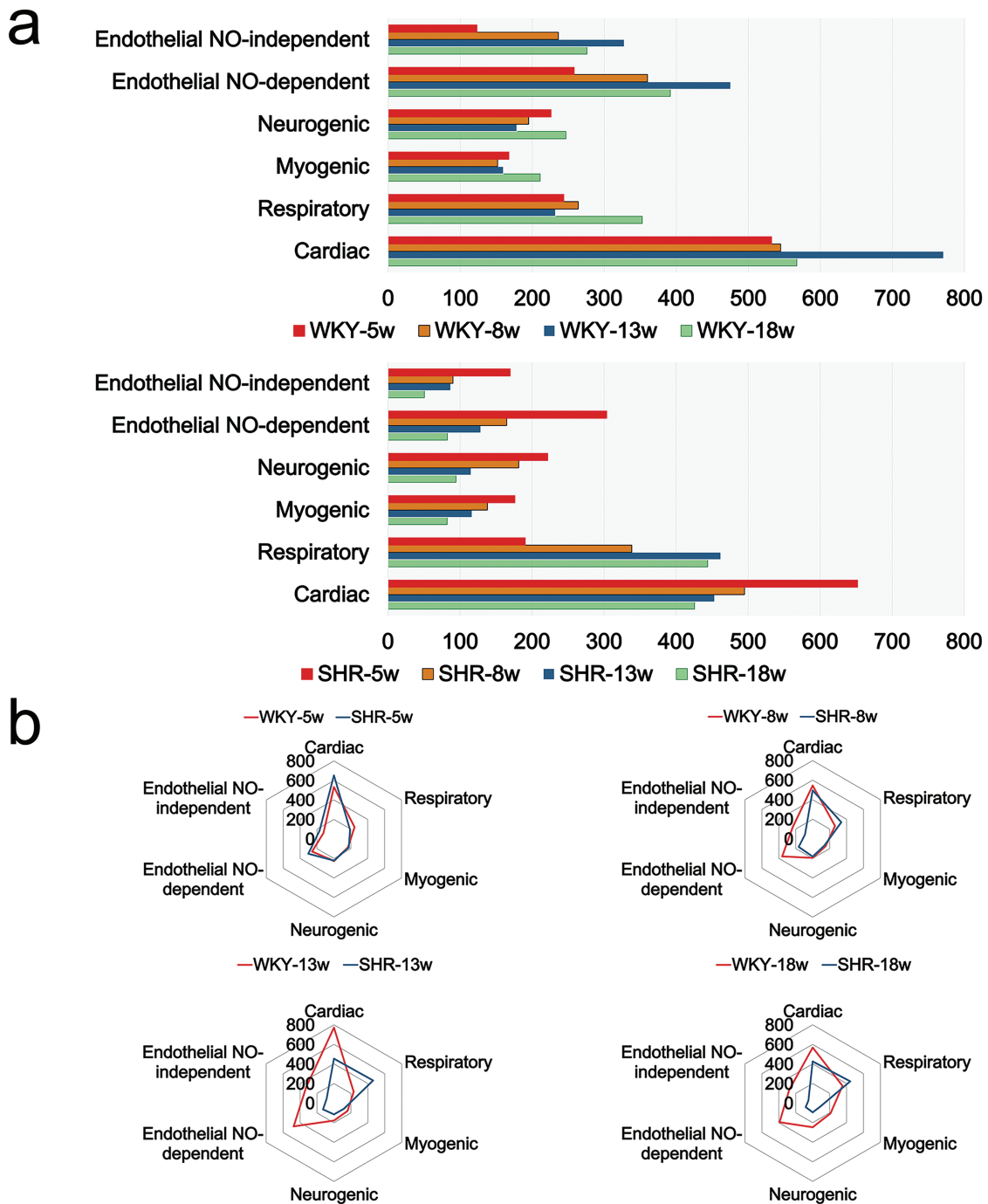


Figure 3. Quantification analyses of characteristic oscillatory amplitudes of pancreatic microcirculation profiles. The combination of laser Doppler flowmetry with wavelet transform signal processing analysis was performed to reveal microcirculatory oscillations related to physiological phenomena. The entire frequency derived from laser Doppler signals was divided into a set of frequency bands, each of which contains a single peak: 0.01–0.015, 0.015–0.04, 0.04–0.15, 0.15–0.4, 0.4–2, and 2–5 Hz, attributed to NO-independent endothelial and NO-dependent endothelial, neurogenic, myogenic, respiratory, and cardiac oscillators, respectively. **(a)** Comparisons of the mean amplitudes of characteristic oscillators in pancreatic microcirculation profiles of WKYs and SHRs at 5, 8, 13, and 18 weeks. **(b)** Radar plots represent varying distributions and differences across amplitudes of characteristic frequency bands corresponding to physiological oscillators. The red line represents amplitudes of WKYs, and the blue line represents amplitudes of SHRs. Abbreviations: SHRs, spontaneously hypertensive rats; WKYs, Wistar Kyoto rats.

Differential pancreatic microcirculatory oscillators in WKYs and SHR

Wavelet transform spectral analysis allows the characterization of physiological oscillators reflecting characteristic activities in pancreatic microcirculation profiles. As illustrated by 3-D scalograms (Figure 2), the time–frequency spectral amplitudes of pancreatic microcirculation profiles revealed the contribution of endothelial oscillators to biorhythmic microhemodynamics in hypertensive and normotensive animals. Furthermore, SHR were noted to exhibit gradually reduced endothelial amplitudes from 8 to 18 weeks, suggesting that endothelial oscillators of pancreatic microcirculation profiles deteriorated during the progression of hypertension.

Comparisons of characteristic oscillators in WKYs and SHR

Since the endothelial oscillators of pancreatic microcirculation profiles deteriorated during the progression of hypertension, the mean amplitudes of NO-dependent and NO-independent endothelial oscillators in SHR and WKYs at 5, 8, 13, and 18 weeks were further analyzed. Notably, the amplitudes of both NO-dependent and NO-independent endothelial oscillators in SHR continuously decreased from 5 to 18 weeks (Figure 3a). Given that microhemodynamic disturbances are the comprehensive pathological microcirculatory phenotype rather than a specific single characteristic oscillator, we then integrated 6 characteristic frequency bands reflecting the changes in oscillators at different ages into radar maps (Figure 3b). The radar maps showed dramatically different amplitude regimens separated by NO-dependent and NO-independent endothelial components between SHR and WKYs. Interestingly, however, no significant change was observed between 5-week-old SHR and WKYs.

Pancreatic microvascular endothelial cell function in WKYs and SHR

As expected, pancreatic microcirculatory blood perfusion showed a positive correlation with endothelial oscillators ($r = 0.3791$, $P = 0.0079$) (Figure 4a). Conversely, endothelial oscillators were negatively related to systolic blood pressure ($r = -0.4552$, $P = 0.0012$) and diastolic blood pressure ($r = -0.4183$, $P = 0.0031$) (Figure 4b). Additionally, the mean amplitudes of NO-dependent and NO-independent endothelial oscillators were significantly reduced in 8-, 13-, and 18-week-old SHR. However, the ratios of NO-dependent to NO-independent endothelial oscillators were similar between SHR and WKYs at all ages. No significant differences were found in NO-dependent or NO-independent endothelial oscillators between the 2 groups of rats in the early stage of hypertension (5 weeks old) (Figure 4c).

To further determine endothelial function in WKYs and SHR, we evaluated plasma nitrite/nitrate and endothelin-1 levels. As shown in Figure 4d, compared with those in WKYs, plasma nitrite/nitrate levels were significantly increased in SHR at 13 and 18 weeks, while no

significant differences were observed in either group in the early stage of hypertension. In addition, as a vasoconstrictor, endothelin-1 was significantly increased in SHR from the prehypertensive to hypertensive stages compared with the normotensive controls. Moreover, the antioxidant status deteriorated, which included significantly increased plasma malondialdehyde levels in SHR and a significant decrease in superoxide dismutase activity in SHR at 5, 8, 13, and 18 weeks. Meanwhile, 5-, 8-, and 13-week-old SHR exhibited elevated inflammatory cytokine interleukin-6 levels.

DISCUSSION

Our current results provide evidence that the pancreatic microcirculation profiles of SHR deteriorate in the prehypertensive stage. Under physiological status, the microcirculation regulates blood distribution and perfusion *via* microvascular vasomotion, avoiding shear forces and high blood perfusion pressure. Capillary rarefaction and small arteriole abnormalities have been observed in hypertensive individuals.²³ In this respect, microcirculatory dysfunction may be closely related to the development of hypertension.²⁴ In the present study, SHR had more divergent pancreatic microcirculatory blood perfusion and distribution patterns than WKYs, which gradually deteriorated from prehypertensive to hypertensive status. Furthermore, the concomitant reduction in microvascular density in hypertensive individuals²⁵ may contribute to decreased blood perfusion and distribution, which would hamper the exchange of metabolic nutrients.

Microvascular vasomotion is one of the essential properties of microcirculation profiles for the maintenance of homeostasis. As expected, hypertensive rats at all ages exhibited abnormal pancreatic microvascular vasomotion, especially damaged microhemodynamics that occurred in the early stage (5 weeks) with normotensive blood pressure, indicating that SHR failed to maintain biorhythmic blood perfusion before the onset of hypertension. The disordered pancreatic microhemodynamics may be considered one of the possible explanations for the disarranged microcirculatory blood distribution pattern. Furthermore, microcirculatory oscillation was affected by vasomotors that stem from intrinsic oscillators of microvessels. As observed in this study, the endothelial oscillators (especially NO-dependent endothelial oscillators), rather than other oscillators, significantly decreased as the hypertensive pathology progressed. Our data favored the view that pancreatic microvascular endothelial cells, which are capable of maintaining microvascular tone²⁶ and modulating inflammation,²⁷ might be the dominant oscillator in abnormal pancreatic microcirculation profiles.

Endothelial nitric oxide synthase (eNOS) is reported to contribute to vasodilation and is related to pathological determinants such as oxidative stress and inflammation.²⁸ NO, synthesized by eNOS, is an endothelial-derived vasodilator, that maintains microvascular endothelial physiological function *via* the nitrate–nitrite–NO pathway.²⁹ It has been reported that the reduction³⁰ and inactivation³¹ of eNOS in hypertensive rats might mediate vasodilatory dysfunction.

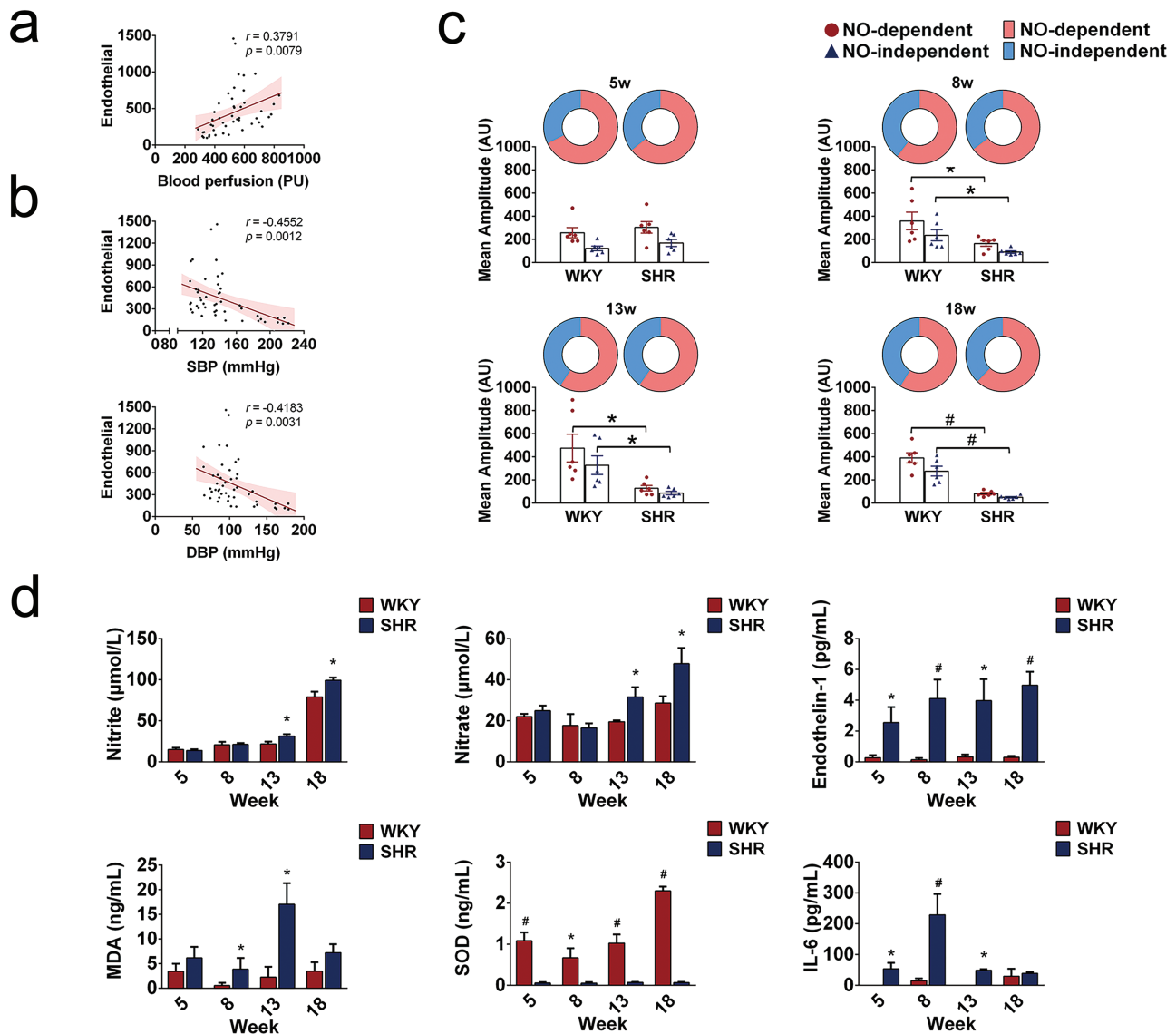


Figure 4. Pancreatic microvascular endothelial cell dysfunction in the progression of hypertension. (a) Correlation between endothelial oscillator and microcirculatory blood perfusion. (b) Correlations between endothelial oscillator and blood pressure. (c) The mean amplitude (AU) of NO-dependent and NO-independent endothelial oscillators in WKYs and SHRs. The ratios of NO-dependent and NO-independent endothelial oscillators are shown in the upper pie chart. Red dots, mean amplitude of NO-dependent endothelial oscillator. Blue triangles indicate the amplitude of the NO-independent endothelial oscillator. (d) The levels of plasma nitrite/nitrate, ET-1, MDA, SOD, and IL-6 in WKYs and SHRs. * $P < 0.05$ compared with WKYs, # $P < 0.01$ compared with WKYs. Abbreviations: DBP, diastolic blood pressure; ET-1, endothelin-1; IL-6, interleukin-6; MDA, malondialdehyde; PU, perfusion unit; SBP, systolic blood pressure; SHRs, spontaneously hypertensive rats; SOD, superoxide dismutase; WKYs, Wistar Kyoto rats.

Consistently, the present study showed a reduction in the amplitudes of NO-independent and NO-dependent endothelial oscillators, together with increased nitrate/nitrite and endothelin-1 levels in SHRs, which may result in a decrease in flow-mediated vasodilation.³² Our data further strengthen the importance of pancreatic microcirculation profiles and endothelial oscillators in hypertension.

With deteriorated endothelial oscillators, microcirculatory hemodynamic balance becomes proconstrictive, prothrombotic, and antifibrinolytic,³³ leading to reactive oxygen species generation³⁴ and inflammatory cytokine synthesis. Elevated levels of plasma nitrite/nitrate over physiological ranges in hypertension are considered

a compensatory response to imbalanced eNOS activity, proinflammatory cytokines, and oxidative stress which are suggestive of the pathogenesis of hypertension.³⁵ These established data are in agreement with our findings; higher levels of malondialdehyde and interleukin-6 and lower levels of superoxide dismutase lead to a reduction in the availability of NO and destabilization of eNOS,³⁶ which might account for the observed development of deteriorated microcirculation profiles.

Whether the microcirculation dysfunction observed in hypertension is the etiological cause or hypertensive effect has been debated for decades and remains controversial. Indeed, it has been documented that the diameter and structure of

small resistance arteries are altered with increased blood pressure, which makes it possible to view microvessel rarefaction as responses to elevated pressure.³⁷ However, there is evidence that microcirculation abnormalities may cause the elevation of blood pressure. For example, renal afferent arterioles were narrowed in the early stage of hypertension in SHR. In addition to the microcirculatory structural evidence, we provided evidence of the occurrence of impaired pancreatic microcirculation profiles in the normotensive and prehypertensive stages in SHR.

In conclusion, our study provides evidence that SHR exhibit abnormal pancreatic microcirculation profiles, including a disarranged pancreatic blood distribution pattern, impaired pancreatic microvascular vasomotion, and reduced amplitudes of endothelial oscillators in the prehypertensive stage and during the progression of hypertension. We believe that focusing on the nature and pathological changes in pancreatic microcirculation profiles will be helpful for enhancing the understanding of microcirculation in hypertension.

FUNDING

We acknowledge the financial support provided by grants from the CAMS Initiative for Innovative Medicine (CAMS-I2M) (No. 2016-I2M-3-006) and the National Natural Science Foundation of China (No. 81900747).

DISCLOSURE

The authors declared no conflict of interest.

REFERENCES

- DALYs GBD, Collaborators H. Global, regional, and national disability-adjusted life-years (DALYs) for 315 diseases and injuries and healthy life expectancy (HALE), 1990–2015: a systematic analysis for the Global Burden of Disease Study 2015. *Lancet* 2016; 388:1603–1658.
- Levy BI, Ambrosio G, Pries AR, Struijker-Boudier HA. Microcirculation in hypertension: a new target for treatment? *Circulation* 2001; 104:735–740.
- De Boer MP, Meijer RI, Wijnstok NJ, Jonk AM, Houben AJ, Stehouwer CD, Smulders YM, Eringa EC, Serné EH. Microvascular dysfunction: a potential mechanism in the pathogenesis of obesity-associated insulin resistance and hypertension. *Microcirculation* 2012; 19:5–18.
- Struijker-Boudier HA, Rosei AE, Bruneval P, Camici PG, Christ F, Henrion D, Lévy BI, Pries A, Vanoverschelde JL. Evaluation of the microcirculation in hypertension and cardiovascular disease. *Eur Heart J* 2007; 28:2834–2840.
- Pradhan RK, Chakravarthy VS. Informational dynamics of vasomotion in microvascular networks: a review. *Acta Physiol (Oxf)* 2011; 201:193–218.
- Liu M, Zhang X, Wang B, Wu Q, Li B, Li A, Zhang H, Xiu R. Functional status of microvascular vasomotion is impaired in spontaneously hypertensive rat. *Sci Rep* 2017; 7:17080.
- Kannenkeril D, Harazny JM, Bosch A, Ott C, Michelson G, Schmieder RE, Friedrich S. Retinal vascular resistance in arterial hypertension. *Blood Press* 2018; 27:82–87.
- DeLano FA, Schmid-Schönbein GW. Proteinase activity and receptor cleavage: mechanism for insulin resistance in the spontaneously hypertensive rat. *Hypertension* 2008; 52:415–423.
- Tran ED, DeLano FA, Schmid-Schönbein GW. Enhanced matrix metalloproteinase activity in the spontaneously hypertensive rat: VEGFR-2 cleavage, endothelial apoptosis, and capillary rarefaction. *J Vasc Res* 2010; 47:423–431.
- DeLano FA, Zhang H, Tran EE, Zhang C, Schmid-Schönbein GW. A new hypothesis for insulin resistance in hypertension due to receptor cleavage. *Expert Rev Endocrinol Metab* 2010; 5:149–158.
- Aragão DS, de Andrade MC, Ebihara F, Watanabe IK, Magalhães DC, Juliano MA, Hirata IY, Casarini DE. Serine proteases as candidates for proteolytic processing of angiotensin-I converting enzyme. *Int J Biol Macromol* 2015; 72:673–679.
- Rodrigues SF, Tran ED, Fortes ZB, Schmid-Schönbein GW. Matrix metalloproteinases cleave the beta2-adrenergic receptor in spontaneously hypertensive rats. *Am J Physiol Heart Circ Physiol* 2010; 299:H25–H35.
- Rosário HS, Waldo SW, Becker SA, Schmid-Schönbein GW. Pancreatic trypsin increases matrix metalloproteinase-9 accumulation and activation during acute intestinal ischemia-reperfusion in the rat. *Am J Pathol* 2004; 164:1707–1716.
- Lindstad RI, Sylte I, Mikalsen SO, Seglen PO, Berg E, Winberg JO. Pancreatic trypsin activates human promatrix metalloproteinase-2. *J Mol Biol* 2005; 350:682–698.
- Chan AHW, Schmid-Schönbein GW. Pancreatic source of protease activity in the spontaneously hypertensive rat and its reduction during temporary food restriction. *Microcirculation* 2019; 26:e12548.
- Schmid-Schönbein GW. An emerging role of degrading proteinases in hypertension and the metabolic syndrome: autodigestion and receptor cleavage. *Curr Hypertens Rep* 2012; 14:88–96.
- Liu M, Zhang X, Li B, Wang B, Wu Q, Shang F, Li A, Li H, Xiu R. Laser Doppler: a tool for measuring pancreatic islet microvascular vasomotion in vivo. *J Vis Exp* 2018; 133:e56028.
- Cracowski JL, Roustit M. Current methods to assess human cutaneous blood flow: an updated focus on laser-based-techniques. *Microcirculation* 2016; 23:337–344.
- Aleksandrin VV, Ivanov AV, Virus ED, Bulgakova PO, Kubatiev AA. Application of wavelet analysis to detect dysfunction in cerebral blood flow autoregulation during experimental hyperhomocysteinaemia. *Lasers Med Sci* 2018; 33:1327–1333.
- Stefanovska A, Bracic M, Kvernmo HD. Wavelet analysis of oscillations in the peripheral blood circulation measured by laser Doppler technique. *IEEE Trans Biomed Eng* 1999; 46:1230–1239.
- Newman JM, Dwyer RM, St-Pierre P, Richards SM, Clark MG, Rattigan S. Decreased microvascular vasomotion and myogenic response in rat skeletal muscle in association with acute insulin resistance. *J Physiol* 2009; 587:2579–2588.
- Smirni S, MacDonald MP, Robertson CP, McNamara PM, O’Gorman S, Leahy MJ, Khan F. Application of cmOCT and continuous wavelet transform analysis to the assessment of skin microcirculation dynamics. *J Biomed Opt* 2018; 23:1–13.
- Tsioufis C, Dimitriadis K, Katsiki N, Tousoulis D. Microcirculation in hypertension: an update on clinical significance and therapy. *Curr Vasc Pharmacol* 2015; 13:413–417.
- Junqueira CLC, Magalhães MEC, Brandão AA, Ferreira E, Cyrino FZGA, Maranhão PA, Souza MDGC, Bottino DA, Bouskela E. Microcirculation and biomarkers in patients with resistant or mild-to-moderate hypertension: a cross-sectional study. *Hypertens Res* 2018; 41:515–523.
- Antonios TF, Singer DR, Markandu ND, Mortimer PS, MacGregor GA. Rarefaction of skin capillaries in borderline essential hypertension suggests an early structural abnormality. *Hypertension* 1999; 34:655–658.
- Vicaut E. Hypertension and the microcirculation. *Arch Mal Coeur Vaiss* 2003; 96:893–903.
- Tsounis D, Bouras G, Giannopoulos G, Papadimitriou C, Alexopoulos D, Deftereos S. Inflammation markers in essential hypertension. *Med Chem* 2014; 10:672–681.
- Förstermann U, Münzel T. Endothelial nitric oxide synthase in vascular disease: from marvel to menace. *Circulation* 2006; 113:1708–1714.
- Victor VM, Nuñez C, D’Ocón P, Taylor CT, Esplugues JV, Moncada S. Regulation of oxygen distribution in tissues by endothelial nitric oxide. *Circ Res* 2009; 104:1178–1183.

30. Kloza M, Baranowska-Kuczko M, Toczek M, Kusaczuk M, Sadowska O, Kasacka I, Kozłowska H. Modulation of cardiovascular function in primary hypertension in rat by SKA-31, an activator of KCa_{2.x} and KCa_{3.1} channels. *Int J Mol Sci* 2019; 20:4118.
31. Peleli M, Zollbrecht C, Montenegro MF, Hezel M, Zhong J, Persson EG, Holmdahl R, Weitzberg E, Lundberg JO, Carlström M. Enhanced XOR activity in eNOS-deficient mice: effects on the nitrate-nitrite-NO pathway and ROS homeostasis. *Free Radic Biol Med* 2016; 99:472–484.
32. Kong X, Li W, Guo LQ, Zhang JX, Chen XP, Liu WY, Yang JR. Sesamin enhances nitric oxide bioactivity in aortas of spontaneously hypertensive rats. *Ther Adv Cardiovasc Dis* 2015; 9:314–324.
33. Rosenblum WI. Endothelium-dependent responses in the microcirculation observed in vivo. *Acta Physiol (Oxf)* 2018; 224:e13111.
34. Diederich L, Suvorava T, Sansone R, Keller TCS 4th, Barbarino F, Sutton TR, Kramer CM, Lückstädt W, Isakson BE, Gohlke H, Feelisch M, Kelm M, Cortese-Krott MM. On the effects of reactive oxygen species and nitric oxide on red blood cell deformability. *Front Physiol* 2018; 9:332.
35. Redón J, Oliva MR, Tormos C, Giner V, Chaves J, Iradi A, Sáez GT. Antioxidant activities and oxidative stress byproducts in human hypertension. *Hypertension* 2003; 41:1096–1101.
36. Kuzkaya N, Weissmann N, Harrison DG, Dikalov S. Interactions of peroxynitrite, tetrahydrobiopterin, ascorbic acid, and thiols: implications for uncoupling endothelial nitric-oxide synthase. *J Biol Chem* 2003; 278:22546–22554.
37. Serné EH, Gans RO, ter Maaten JC, Tangelder GJ, Donker AJ, Stehouwer CD. Impaired skin capillary recruitment in essential hypertension is caused by both functional and structural capillary rarefaction. *Hypertension* 2001; 38:238–242.
38. Nørrelund H, Christensen KL, Samani NJ, Kimber P, Mulvany MJ, Korsgaard N. Early narrowed afferent arteriole is a contributor to the development of hypertension. *Hypertension* 1994; 24:301–308.